Mechanistic Model Describing the Uptake of Chemicals by Aquatic Integrative Samplers: Comparison to Data and Implications for Improved Sampler Configurations

Satoshi Endo, Yunosuke Matsuura, Etiënne L. M. Vermeirssen

Mechanistic Model Describing the Uptake of Chemicals by Aquatic Integrative Samplers: Comparison to Data and Implications for Improved Sampler Configurations

Satoshi Endo,[†,*] *Yunosuke Matsuura,*[†] *Etienne Vermeirssen*[‡]

†Graduate School of Engineering, Osaka City University, Sugimoto 3-3-138, Sumiyoshi, 558-8585 Osaka, Japan

‡Swiss Centre for Applied Ecotoxicology Eawag-EPFL, Überlandstrasse 133, CH-8600 Dübendorf, Switzerland

*Corresponding author:

Phone/Fax: ++81-6-6605-2763

satoshi.endo@eng.osaka-cu.ac.jp

TOC Art

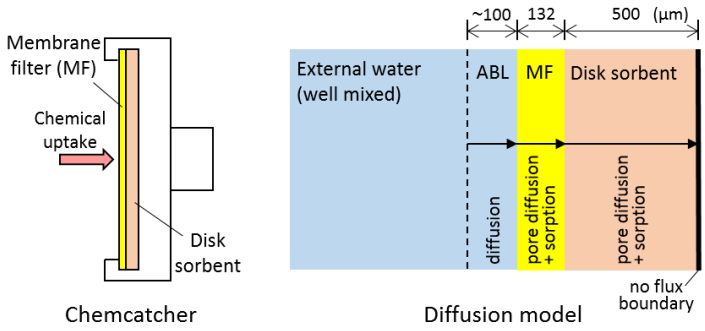
Membrane filter (MF)
Chemical uptake
Disk sorbent
Chemcatcher
~100
132
500 (µm)
External water (well mixed)
ABL
MF
Disk sorbent
diffusion
pore diffusion + sorption
pore diffusion + sorption
no flux boundary
Diffusion model

Abstract

Aquatic integrative passive samplers are used for determining aqueous concentrations of polar organic pollutants, yet their uptake mechanisms are poorly understood. We introduce a one-dimensional model to simulate uptake by a passive sampler, Chemcatcher. The model considers the uptake as molecular diffusion through a series of the aqueous boundary layer (ABL), the membrane filter (MF), and the sorbent disk with concurrent sorption by matrix of the MF and the disk. Uptake profiles of ca 20 polar chemicals measured over a week and a month were accurately modeled. Characteristic behavior such as lag-times, linear and curved uptake, and equilibrating behavior were well-explained by the model. As the model is mechanistically based, it was able to show the combined influences of the MF/water ($K_{MF/w}$) and disk/water ($K_{disk/w}$) partition coefficients, diffusion coefficients, and the ABL thickness on the sampling rates. On the basis of the model results, we offer three concrete recommendations to achieve linear uptake needed for measuring time-weighted average concentrations: (i) Use a MF that does not significantly sorb chemicals (e.g., log $K_{MF/w} < 3$) to avoid lag times. (ii) Use a sorbent with strong sorption properties (e.g., log $K_{disk/w} > 6$) for effective trapping of chemicals on the disk top layer. (iii) Make the ABL and/or the MF thicker so that the diffusion toward the disk slows down.

Introduction

Aquatic integrative passive samplers such as Chemcatcher[1] and polar organic chemicals integrative samplers (POCIS)[2] have been investigated intensively in the past decades. These samplers contain sorbent material such as Empore SDB extraction disks and Oasis HLB solid phase extraction sorbent and are covered with a diffusion limiting membrane filter (MF). Once the sampler is deployed in water, chemicals dissolved in water permeate through the MF and accumulate in the sorbent. Then, the mass of a chemical in the sorbent is measured, from which the time-weighted average (TWA) concentration in water over the deployment time is derived. The possibility of measuring TWA concentrations in a relatively simple manner is a major reason that these types of passive samplers have received particular attention by environmental scientists and increasingly by regulators.

In the current practice, the mass of the chemical sorbed by the sorbent, M_{sorb} [μg], is often related to the external water concentration using the linear uptake (or sampling rate) model.[1,3] This model appears,

$$M_{\mathrm{sorb}} = R_{\mathrm{s}} t C_{\mathrm{TWA}} \qquad (1)$$

where R_{s} is the sampling rate [L/d], t is the time after the deployment of the sampler [d], and C_{TWA} is the TWA concentration in external water [μg/L]. Following eq 1, C_{TWA} can be obtained from M_{sorb} using an empirically determined value of R_{s}. So far, much effort has been devoted to experimental determination of R_{s} values.[4,5] Developing an empirical prediction method of R_{s} for untested chemicals has been attempted,[5-7] yet there is not a generally accepted prediction method. The fundamental reason for this may be that we still lack mechanistic understanding regarding the processes that determine R_{s}.

While the measurement concept as presented above is rather simple, it has been debated how accurately the currently used passive samplers can measure C_{TWA} in the field.[8] For example:

according to eq 1, if the external water concentration is constant, M_{sorb} should increase linearly with time. This is however not always the case. The M_{sorb} vs t plot often shows a concave downward curve (i.e., decreasing slope).[9] In the literature, this behavior is modeled with a first-order model,[3]

$$\frac{dM_{\mathrm{sorb}}}{dt} = k'\left(C_{\mathrm{w,ex}} - \frac{C_{\mathrm{sorb}}}{K_{\mathrm{sorb/w}}}\right) \quad (2)$$

$C_{w,ex}$ is the concentration in external water [µg/L], C_{sorb} is the concentration in the sorbent [µg/kg], $K_{sorb/w}$ is the sorbent/water partition coefficient [L/kg], and k' is the first-order rate constant [L/s]. The time integral of eq 2 under a constant $C_{w,ex}$ condition can fit to asymptotic (equilibrating) behavior of measured uptake profiles. This type of model may be extended to multi-compartment models that include the MF as an additional compartment.[10] Three-compartment models were shown to fit to the data that show lag-time behavior,[9] which is often observed with chemicals that sorb strongly to the MF.[9,11,12]

While compartment models fit the data well, such models are not based on physico-chemical processes that occur during the chemical uptake by currently used passive samplers. Compartment models consist of a suite of well-mixed phases that are interconnected by the respective exchange rates. Hence, if the actual phases of the sampler are not well-mixed, it is unclear what the fitted rate constants and related partition coefficients physically mean. The lack of a solid mechanistic basis does not allow these models to be used for predictive purposes. Moreover, the model results and fitted parameters do not tell us how R_s is related to chemical and material properties. Better mechanistic understanding is urgently needed to identify the conditions required for the ideal linear uptake that allows accurate measurement of C_{TWA}, to establish R_s prediction methods, and to account for influences of environmental conditions on R_s.

This work introduces a mechanistically based, one-dimensional (1D) diffusion model for porous media to describe the chemical uptake behavior of Chemcatcher. The MF and the sorbent disk are both porous materials, consisting of solid matrices which sorb chemicals and water-filled

pores through which chemicals can diffuse. Such a diffusion model is often used in environmental science to capture the solute transport in subsurface and sediment (ref 13, pp 544-545) and has also been used for the passive sampling behavior of metals by diffusive gradients in thin films (DGT) devices.[14,15] In a previous study, we successfully applied this type of model to characterize the permeation of chemicals through MFs.[16] Interestingly, although integrative passive samplers rely on passive diffusion of chemicals for their sampling, none of the previous models for Chemcatcher and POCIS explicitly considers diffusion processes within the devices. In this contribution, we explain the modeling concept, compare the modeling results to experimental data, and discuss how model parameters influence the uptake behavior of the samplers. Finally, recommendations are offered for improved sampler configurations that allow to measure C_{TWA} for a broader range of chemicals.

Methods

Model. The basic modeling concept of this work is that the chemical uptake by integrative passive samplers is considered as 1D-diffusive transport through the aqueous boundary layer (ABL), the MF, and the sorbent (Figure 1). The equation that governs the diffusion process is,

$$\frac{\partial C_w}{\partial t} = \frac{D_e}{\alpha}\frac{\partial^2 C_w}{\partial x^2} \qquad (3)$$

C_w is the porewater concentration. D_e is the effective diffusion coefficient in the MF or in the sorbent layer [m^2/s], estimated as $D_e = D_w \varepsilon/\tau^2$ where D_w is the aqueous diffusion coefficient [m^2/s], ε is the porosity [-], and τ is the tortuosity [-]. α is the capacity factor [-] defined as $\alpha = \varepsilon + \rho K_{j/w}$ with ρ being the bulk density [kg/L] and $K_{j/w}$ either the MF/water or the sorbent/water partition coefficient [L/kg]. Here, local equilibrium and linear isotherms for the sorption by MF and sorbent solid phases are assumed. x [m] is the position in the axis perpendicular to the MF and sorbent layers. For ease of computation, it is assumed that the linear concentration gradient is instantaneously established in the

ABL, as the time needed for this process (typically seconds to minutes) is much shorter than the time-scale of passive sampling experiments. Thus,

$$Flux_{ABL} = k_{ABL}\left(C_{w,ex} - C_{w,x=0}\right) \quad (4)$$

where $Flux_{ABL}$ is the flux of the chemical through the ABL and $C_{w,x=0}$ is the aqueous phase concentration at the ABL-MF interface. k_{ABL} is the mass transfer coefficient [m/s] and is equal to D_w/d_{ABL} (d_{ABL}, the thickness of the ABL [m]). We assume that d_{ABL} is independent of the chemicals of concern, which is a valid approximation for typical environmental chemicals, as shown before.[16] The no-flux boundary condition was set at the back end of the sorbent disk.

Eq 3 was solved by the finite difference method with a centered difference approximation for space and Euler's explicit method for time using *R* software, as described previously.[16] The grid size Δx was 2 μm and the time increment Δt was varied so that the condition of $(\Delta t\, D_e/\alpha)/(\Delta x)^2 < 1/2$ was fulfilled in order to avoid numerical problems.

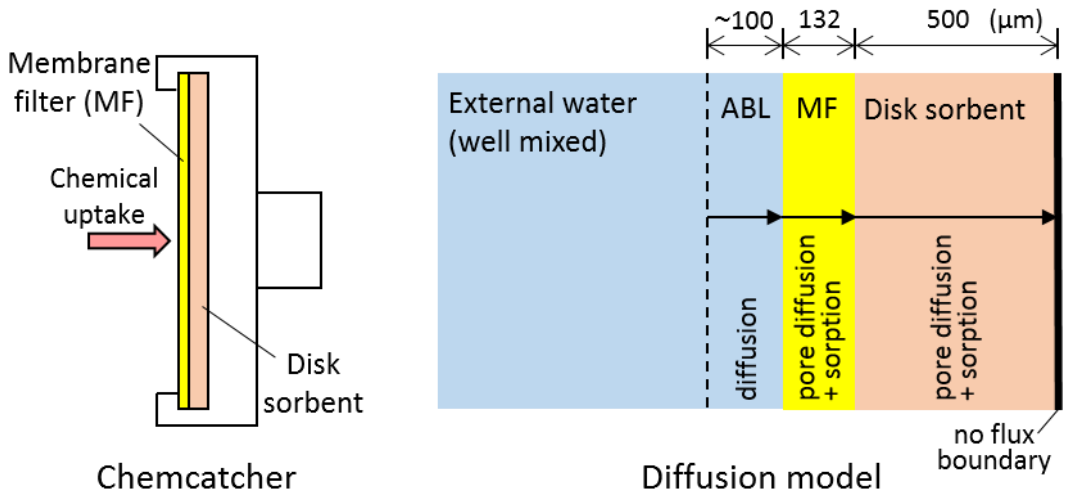

Figure 1. A typical configuration of Chemcatcher and the conceptual model for chemical uptake. The scales are given as examples.

Data. To test the modeling concept and calibrate some parameters, we used the measured data for the uptake of 22 chemicals by Chemcatcher reported by Vermeirssen et al.[9,17]

In ref [17], Chemcatchers with Empore SDB-RPS disks (3M, St Paul, MN) were deployed in a "naked" configuration (without MF) in a channel system for 8 d (mean temperature, 13 °C; flow rate 0.08 – 0.10 m/s). In a separate experiment, samplers of the same type were placed in a circular tank for 25 d (26 °C; 0.12 – 0.14 m/s). Concentrations of the 22 chemicals in water were adjusted to ca. 1 or 0.4 μg/L and were regularly monitored, and the mass sorbed by the disk was measured over time. These time-resolved uptake data for naked Empore disks offer the possibility to characterize the sorption properties of the disks without being influenced by MF.

In ref 9, Empore SDB-RPS disks were each covered with a PES filter (Supor 100 membrane disk filter, 0.1 μm, Pall Corporation, NY), i.e., a standard Chemcatcher format. These devices were deployed in the same channel system (0.08 ± 0.015 m/s) for 6 d (20.5 °C) or 32 d (13.8 °C). The amounts sorbed by the PES MF and by the SDB-RPS disks were monitored over time.

Parameters. Parameter values used for modeling are as following: Porosity ε, 0.7 (PES filter) and 0.5 (Empore disk); tortuosity τ, 1.3 (both PES and Empore disk); bulk density ρ, 0.372 kg/L (PES filter) and 0.424 kg/L (Empore disk); thickness d_{MF}, 132 μm (PES filter) and d_{disk}, 500 μm (Empore disk). Out of these, ε, d_{MF}, and d_{disk} are provider-stated values, while τ and ρ are our estimates. For more details, see the Supporting Information (SI), SI-1. For mass calculations, a cross sectional area (A) of 12.57 cm^2 was used, which is calculated from the exposed diameter of 40 mm. Disks and MF were actually 47 mm and partially covered in the sampler body; we ignored lateral diffusion within the MF and the disk. D_w at 25 °C was calculated from its dependence on McGowan's molar volume of the chemical (ref 13, p 538). Temperature dependence of D_w was estimated following Zhang and Davison's approach.[18] $K_{PES/w}$ values determined by batch experiments[9] were used as starting values. In contrast, experimental $K_{disk/w}$ are unavailable, and thus estimated here by model fitting (see below).

Results and Discussion

Modeling Uptake by Naked Empore Disks. For modeling the chemical uptake by naked Empore SDB-RPS disks, we need estimates for d_{ABL} and $K_{disk/w}$. The former is common for all chemicals and the latter is specific to each chemical. As explained in detail in the Supporting Information (SI-2), the initial uptake behavior for strongly sorbing chemicals ($\log K_{disk/w} \geq 6$) is sensitive to d_{ABL} but not to $K_{disk/w}$. Making use of this characteristic behavior, we adjusted the value of d_{ABL} using four chemicals with high expected $K_{disk/w}$ (diazinon, irgarol, metolachlor, terbutryn). The $K_{disk/w}$ values for these chemicals were initially set to 10^6 L/kg and the model was run with varying d_{ABL} values to minimize the sum of squared residuals (SSR) between modeled and experimental mass sorbed by the disk (M_{disk}). Only the data for the first 24 h were used for this purpose. The optimal values for d_{ABL} were 73–91 μm and 50–59 μm for the 8-d channel experiment and the 25-d tank experiment, respectively. The mean values were 80.7 and 52.8 μm. These values are well within an expected range for flowing conditions.[19,20] A thicker ABL for the 8-d channel experiment than the 25-d circular tank experiment was expected, because the flow rate of the former experiment was slightly lower (0.08–0.10 vs 0.12–0.14 m/s), and the former experiment placed the naked Empore disk in a 20 mm deep pocket whereas the latter experiment did not. We set d_{ABL} to 80 and 52 μm for the 8 d and 25 d experiments, respectively, for further calculations. Note that the obtained d_{ABL} would be only slightly different if another $K_{disk/w}$ were used. For instance, with $K_{disk/w} = 10^7$ L/kg, one would obtain a mean d_{ABL} value of 86.8 and 61.3 μm, respectively.

With d_{ABL} obtained above, the model without the MF was run. $K_{disk/w}$ was adjusted for each chemical and experiment. With $K_{disk/w}$ adjusted, the model was able to reproduce the experimental data well (Figure 2A; all results in SI-3). Note that 3 of the 22 chemicals (benzotriazole, 5-methylbenzotriazole, caffeine) showed irregular uptake data in the 25 d experiment, as also discussed

in ref [17], and were not further considered in this work. The log $K_{disk/w}$ values obtained from the 8 d and 25 d experiments are similar and line up straight in the 1:1 plot (SI-4). Log $K_{disk/w}$ for 25 d is only insignificantly (0.11±0.21) higher than those for 8 d, indicating high consistency. All these results suggest that the 1D diffusion model with calibrated K_{disk} can describe the chemical uptake by Empore disks.

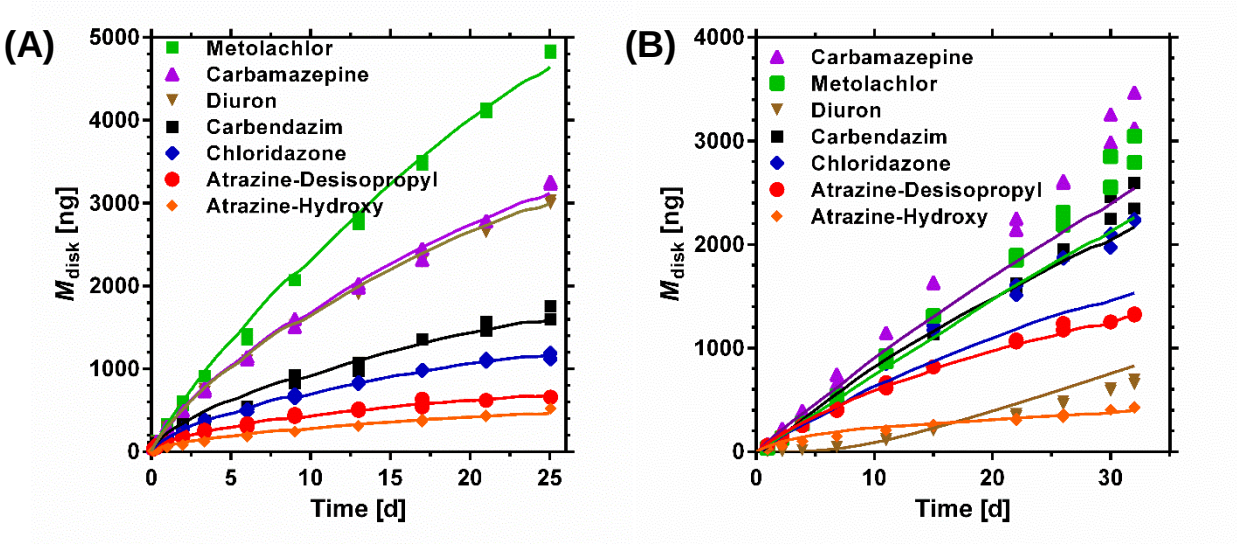

Figure 2. Modeling the uptake of chemicals by naked Empore disks (A) and the whole Chemcatcher (B). Data points in panel A are from the 25 d experiment in ref [17] and data points in panel B are from the 32 d experiment in ref 9. Lines are the model results (see the text).

Modeling Uptake by Chemcatcher. Now we run the model with both MF and the disk involved and compute the uptake of chemicals by the whole Chemcatcher device. The $K_{disk/w}$ values used were those obtained from 8 d experiments above (because values are available for all 22 chemicals) and the $K_{PES/w}$ values used were from ref 9 (measured by batch experiments conducted in the laboratory). The d_{ABL} value was fixed to 80 μm, considering the similar channel system as above. Thus, in this first attempt, we did not fit any parameter to the data with which to evaluate the model.

The calculated M_{disk} over time generally agreed with the experimental data (Figure 2B; all results are shown in SI-5). Since no fitting was done this case, it is not surprising that some differences exist between calculated and experimental M_{disk}. Still, the differences are mostly within 10%. The model prediction also captured the more challenging scenarios for uptake behavior such as the response to a peak concentration of benzotriazole and the initial lag-phases of diazinone and diuron. Nevertheless, there are two types of discrepancy found for the 32 d experiment data. First, M_{disk} of the two most weakly sorbing chemicals (sulfamethoxazole, sulcotrione) was underpredicted by up to a factor of 2. As both chemicals are anionic, difference in $K_{disk/w}$ due to the varied water chemistry (i.e., pH, salts) may be a likely reason. Second, while M_{disk} was well predicted, the mass in the PES filter (M_{PES}) was generally underpredicted by the model by up to a factor of 5 (SI-5). Likely, the values of $K_{PES/w}$ used were too low for the 32 d data. Temperature difference between the laboratory (room temperature, 20–25 °C) and the channel system (13.8 °C) might have caused differences in $K_{PES/w}$. It is important to note that this inaccuracy in $K_{PES/w}$ does not influence the model results for M_{disk} if the sorption of the PES filter is weak. Only if $K_{PES/w}$ is high and M_{PES} amounts to a level comparable to M_{disk} (e.g., for chloridazon, diazinon), does the value of $K_{PES/w}$ influence M_{disk} predictions. To test if $K_{PES/w}$ could be a reason for the model inaccuracy, we adjusted the $K_{PES/w}$ value for each compound by minimizing the SSR for M_{PES} (data not shown). This adjustment, of course, improved the agreement between calculated and experimental M_{PES} for all compounds and did not cause an appreciable change in calculated M_{disk} for low $K_{PES/w}$ compounds, while it also improved the calculated M_{disk} for high $K_{PES/w}$ compounds.

In SI-4, we compared $K_{disk/w}$ and $K_{PES/w}$ obtained from the model fitting explained above, $K_{PES/w}$ from batch experiments, and octanol-water partition coefficients (K_{ow}). Several remarks can be offered: (1) The $K_{PES/w}$ values obtained from the 6 d and 32 d experiments closely agree (difference: 0.12 ± 0.32 log units (mean ± SD) or a factor of 1.3). (2) These 6 d and 32 d $K_{PES/w}$ values tend to be higher than $K_{PES/w}$ from batch experiments (difference: 0.38 ± 0.24 log units (a

factor of 2.4) and 0.25 ± 0.43 log units (a factor of 1.8), respectively), as also discussed in ref 9. (3) $K_{disk/w} \geq K_{PES/w}$ by 0–3 log units, and the correlations between log $K_{disk/w}$ and log $K_{PES/w}$ are only moderate (R^2 = 0.60–0.69). (4) So are the correlations between log $K_{disk/w}$ and log K_{ow} (R^2 = 0.66, 0.88) and between log $K_{PES/w}$ and log K_{ow} (R^2 = 0.39, 0.46). Besides, $K_{disk/w} > K_{ow}$ by 2–4 log units, and $K_{PES/w} \geq K_{ow}$ by 0–3 log units. The sorption by PES can be strong, as reported previously,[16] and comparable to that of the Empore SDB-RPS disk and octanol.

General Uptake Curve for Chemcatcher. For better qualitative understanding on how characteristics of uptake curves are associated with diffusion processes in the sampler, we divide the uptake profile into four phases: (1) lag phase, (2) linear phase, (3) curve phase, and (4) equilibrium phase (Figure 3). Note that, for simplicity, the exposure concentration is set constant in this discussion.

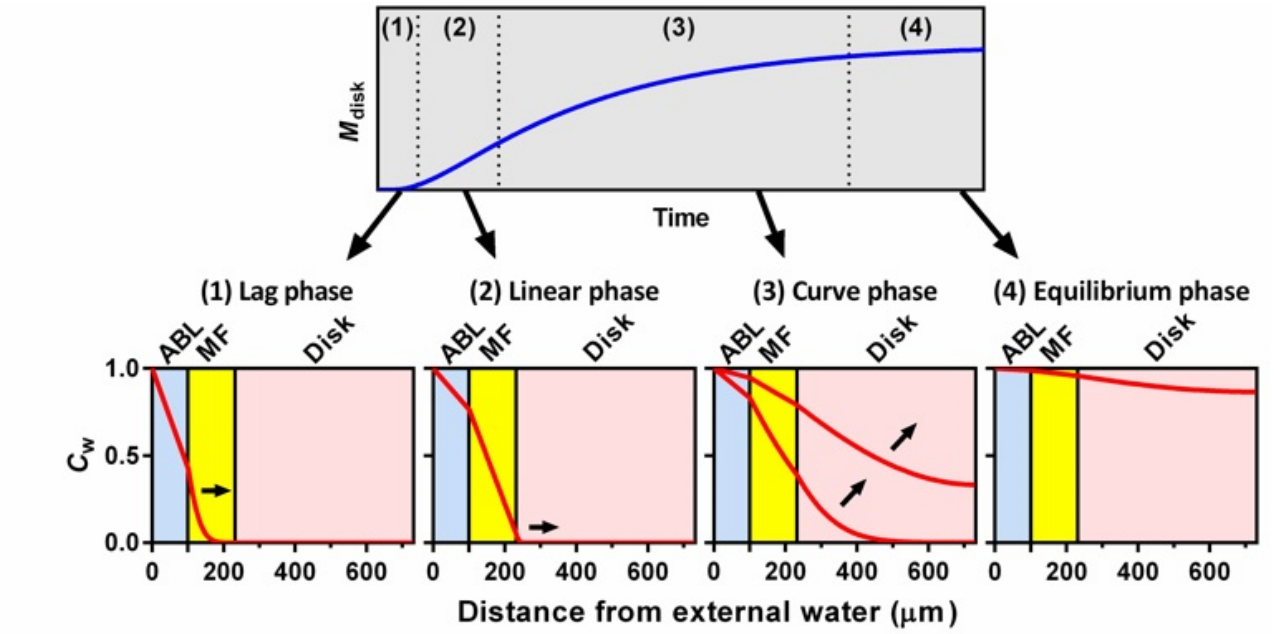

M_{disk}	≈ 0	Linear increase	Curved increase	Plateau
Uptake rate	≈ 0	Highest, constant	Middle to low, decreasing	≈ 0
Concentration front	Advancing within MF	In the top layer of disk	Advancing within disk	Having reached the back end of disk
$M_{disk}/M_{disk,eq}$	≈ 0	< 0.01	0.01–0.9	0.9–1
Key property for occurrence	High $K_{MF/w}$	High $K_{disk/w}$	Low $K_{disk/w}$	Very low $K_{disk/w}$

Figure 3. General uptake curve and pore water concentration profiles for Chemcatcher. C_w is the (pore) water concentration. $M_{disk}/M_{disk,eq}$ means the degree of sorption equilibrium in disk. Note that the uptake curve presented here is shown for illustration purpose and does not reflect a real case.

In the lag phase, the chemical is transferred from external water through the ABL and is effectively trapped by the MF. The diffusive concentration front moves from the water-exposed surface of MF toward its interior, and this phase ends when the concentration front reaches the back side of the MF. M_{disk} virtually stays 0 (no uptake by the disk). In the linear phase, the diffusing chemical is captured by the top layer of the disk. In this phase, the steady-state concentration

gradient from external water through the ABL and the MF pore water defines the uptake rate (slope), which is equal to the following expression.

$$\frac{D_w A \varepsilon_{MF} C_{w,ex}}{d_{ABL}\varepsilon_{MF} + d_{MF}\tau_{MF}} \quad (5)$$

This rate represents the fastest uptake (highest slope) in the entire deployment time. As the concentration front advances toward the inside of the disk, the linear phase shifts to the curve phase. The uptake rate decreases because the diffusive path length from the source (external water) increases and the gradient becomes gentler. As the concentration gradient becomes gentler and gentler, the uptake rate becomes lower and lower, and the system finally approaches the sorption equilibrium. Note that, before these four phases, there could be a preceding phase where the steady-state diffusion is being established in the ABL. As mentioned above, this process is generally quick and thus not considered here.

Depending on the chemicals, the sampler materials, and the environmental conditions, not all of the four phases will appear in uptake experiments. Rather, it may be usual that only one or two phases dominate the entire sampling time. For example, the lag phase is significant only if the MF/water partition coefficient ($K_{MF/w}$) is sufficiently high. With strong sorption by the disk (i.e., high $K_{disk/w}$), an extended time for the linear phase is expected, because the top layer of the disk virtually catches all chemicals. With relatively low $K_{disk/w}$, in contrast, the diffusion concentration front quickly advances into the disk, and as a result, the linear phase is not visible, and the curve phase prevails. If $K_{disk/w}$ is very low, the sampler reaches equilibrium within the deployment time. More quantitative discussions are given in the next sections.

Influences of Sorption Properties on the Uptake Profile. In this and the next section, we discuss the influences of various parameters on the uptake of chemicals by Chemcatcher. Figure 4 compares the uptake of hypothetical chemicals with varying $K_{MF/w}$ and $K_{disk/w}$ within 14 d, simulated with the 1D diffusion model presented above. For these calculations, we used the same values for *d*,

ε, and τ for the MF and the disk as above (see SI-1). Additionally, D_w was set to 6×10^{-10} m^2/s, d_{ABL} to 100 μm, and $C_{w,ex}$ to 1 μg/L. These values are considered the standard set here.

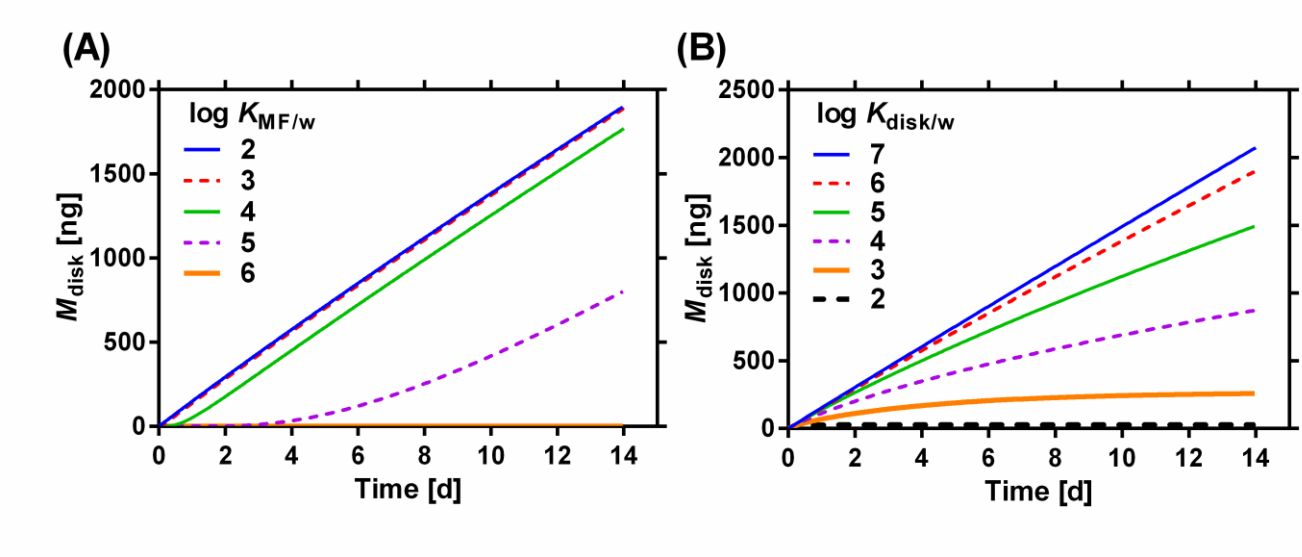

Figure 4. Dependence of the Chemcatcher uptake on the partition coefficients. (A) Dependence on log $K_{MF/w}$. Log $K_{disk/w}$ is fixed to 6. (B) Dependence on log $K_{disk/w}$. Log $K_{MF/w}$ is fixed to 2. In all cases, d_{ABL} = 100 μm, $D_w = 6 \times 10^{-10}$ m^2/s, and $C_{w,ex}$ = 1 μg/L. The other parameters are presented in SI-1.

As Figure 4A shows, if log $K_{MF/w} < 4$, variation of $K_{MF/w}$ has little influence on the uptake behavior. A higher $K_{MF/w}$ would cause a substantial lag time (> 1 d) and reduce M_{disk} throughout. Apparently, there needs to be a breakthrough of the MF before M_{disk} appreciably increases. This result is consistent with the lag-time behavior reported in the literature[9,11,21-23] and additionally offers mechanistic explanations and a quantitative suggestion as to how low $K_{MF/w}$ should be.

Figure 4B shows that the uptake is also sensitive to $K_{disk/w}$. Generally, the higher the $K_{disk/w}$ value, the faster and the more linear the uptake. This trends holds true up to log $K_{disk/w}$ = 6, above which the uptake is just linear and no longer dependent on $K_{disk/w}$ within 14 d. Even with log $K_{disk/w}$ = 5, the uptake can be considered linear within the first few days. As explained in the previous section,

with sufficiently high $K_{disk/w}$, the top layer of the disk effectively traps all incoming chemicals and the uptake is simply determined by the steady-state diffusion through the ABL and the MF (i.e., linear phase). In contrast, if log $K_{disk/w}$ = 3–5, the uptake profile is curved (i.e., curve phase), and if log $K_{disk/w}$ < 3, the disk quickly reaches sorption equilibrium (i.e., equilibrium phase).

Simulation of "Experimental" R_s. In the literature, it was repeatedly shown that experimentally determined R_s values are not a simple function of physico-chemical properties of chemicals.[4,6,7,24] This may not be surprising, considering the fact that the overall uptake behavior is controlled by multiple processes, each of which is influenced by more than one parameter. To shed light on the interrelations of various parameters in determining R_s, we simulated "experimental" R_s using our model. The model was run with different sets of parameter values, and M_{disk} at 3, 7, 10, and 14 d were calculated. Then, simple regression with zero intercept (eq 1) was computed for these M_{disk} data to obtain R_s.

Figure 5A shows the dependence of the resulting R_s on $K_{MF/w}$ and $K_{disk/w}$. The parameters other than the partition coefficients were the same as above (i.e., the standard set). Note, we did not simulate cases where $K_{MF/w} > K_{disk/w}$ by a factor of 10 or more, because experimental data suggest $K_{MF/w} \leq K_{disk/w}$ as shown above. The R_s values are highest where $K_{MF/w}$ is low and $K_{disk/w}$ is high (right bottom of Figure 5A). In this condition, a lag time does not occur, while a desirable, extended linear uptake profile is achieved (i.e., the linear phase dominates). With decreasing $K_{disk/w}$, R_s decreases because of increasing diffusion path length over time (i.e., the curve phase occurs). Moving upward in the figure, R_s decreases with increasing $K_{MF/w}$, as a result of sorption to the MF (i.e., the lag phase). Particularly, R_s rapidly decreases around $K_{MF/w}$ of 4–5 on the log scale, as also seen in Figure 4. It should be noted that the curve linearity to derive R_s deteriorates if $K_{disk/w}$ is low or $K_{MF/w}$ is high, as shown with R^2 in Figure 5B, because the curve shows a lag-time in the former case and plateauing behavior (equilibrium) in the latter case. Overall, these plots clearly indicate the problems of high $K_{MF/w}$ and low $K_{disk/w}$ when TWA concentrations need to be measured.

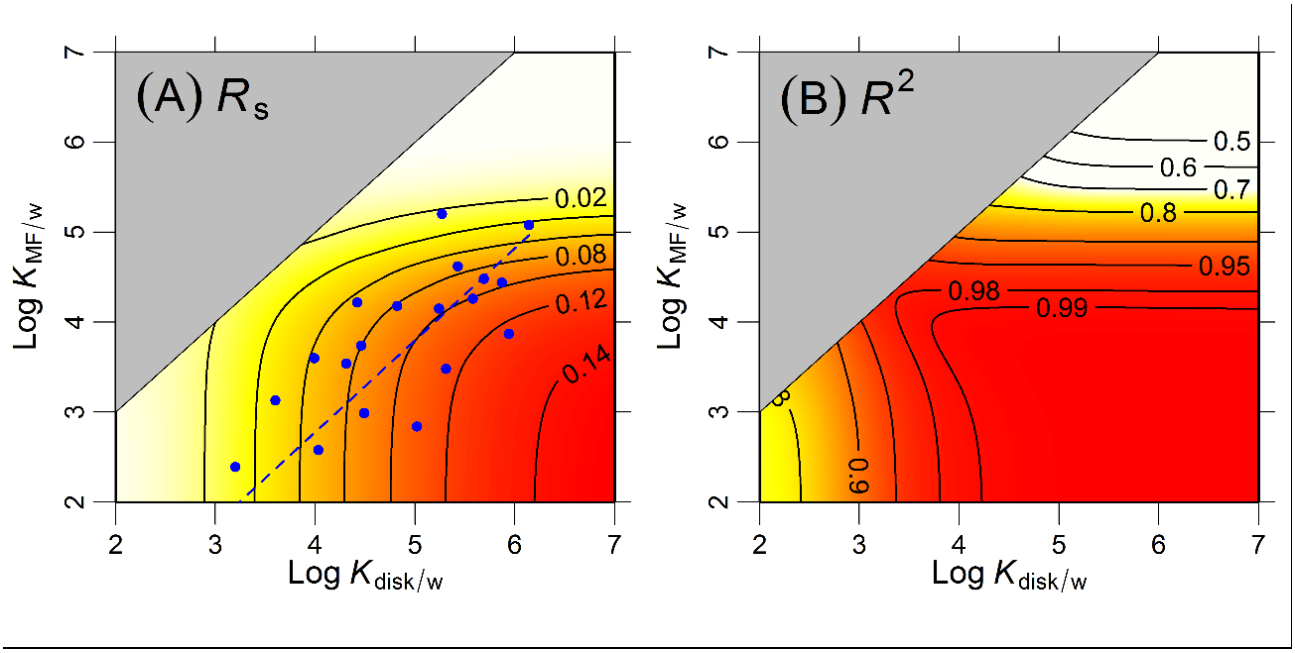

Figure 5. Simulated "experimental" R_s as a function of log $K_{MF/w}$ and log $K_{disk/w}$ (A) and R^2 of the linear regression to derive R_s (B). Model simulations were performed for every half log units of partition coefficients, and the space between these grid points was interpolated using *R* software (package *field*, function *image.smooth()*). Data points are K_{PES} and K_{disk} values estimated in this work for the 22 chemicals used by Vermeirssen et al.[9,17] (but three chemicals are out of scale). The dashed line indicates the linear regression. Note that the grey area ($K_{MF/w}$ > 10 $K_{disk/w}$) was not modeled.

From the contour plot in Figure 5A, we can speculate why previous studies on passive samplers suggested a linear, a polynomial or no relationship between R_s and log K_{ow}.[4,5,25,26] The dots in Figure 5A indicate 22 compounds used by Vermeirssen et al., showing that their regression line diagonally crosses the contour lines. As discussed above, log $K_{PES/w}$, log $K_{disk/w}$, and log K_{ow} for this data set are moderately correlated with each other. Thus, from Figure 5A, we can say that R_s is low when log K_{ow} is low, increases with log K_{ow} up to some point, and decreases toward higher log K_{ow}, i.e., a polynomial relationship. It would not be any surprise if another study finds a linear or no

relationship between R_s and log K_{ow}, because the correlations between the partition coefficients are weak (see SI-4) and thus the regression line depends on the data sets.

In SI-6, the same type of plots generated with varying d_{ABL} (50, 100, 200, 1000 μm) and D_w (3, 6, 12 × 10^{-9} m^2/s) are presented. Comparing d_{ABL} of 50, 100, and 200 μm, it appears that a factor 2 difference in d_{ABL} would cause only 20 % difference in R_s in linear uptake cases. This result suggests that a change in flow regime, which influences d_{ABL}, would not have a major influence on R_s as far as d_{ABL} is in a typical range (50–200 μm in flowing conditions).[19,20] With d_{ABL} = 1000 μm (a stagnant water condition), R_s reduces to 30–40% of that with d_{ABL} = 100 μm. In contrast, D_w has nearly quantitative influences on R_s, i.e., a factor of 2 variation in D_w changes R_s by a factor of ca 2 in linear uptake cases. A change in D_w by a factor of 2 roughly corresponds to a temperature change by 20 degrees.

Recommendations for Achieving Linear Uptake. To measure TWA concentrations with passive samplers, it is imperative that the uptake profile is linear. On the basis of the model simulations presented above, we offer three suggestions for realizing ideal linear uptake by passive samplers.

First, MF should not significantly sorb the chemical. To avoid a lag-time > 1 h, log $K_{MF/w}$ should be < 3 in the standard Chemcatcher setting. As discussed previously,[16] sorption by PES is often strong and thus can cause a lag-time problem. PTFE membrane filters may be a useful alternative, as sorption by PTFE is generally weak.[16] In terms of no lag time, passive samplers without a MF could also be an option, although risks of fouling and damages increase, and R_s becomes generally higher and more susceptible to the variations of d_{ABL}. Moreover, with increasing R_s, the period of linear uptake would be shortened.

Second, partitioning to the sorbent disk should be very strong to minimize the diffusion into the inner part of the sorbent pack. For example, log $K_{disk/w}$ should be > 6 in the standard Chemcatcher

setting to have linear uptake over 2 weeks. $K_{disk/w}$ should be so high because only the top layer of the disk can contribute to the linear uptake. Increasing the amount of sorbent (i.e., increasing the disk thickness) does not help to maintain uptake in the linear phase. Introducing a stronger sorbent such as carbon-based sorbent instead of polymer-based may increase $K_{disk/w}$ and thus lead to a longer linear uptake phase. Note, however, that extremely strong sorbent such as activated carbon may cause a problem of low recovery of sorbed chemicals by solvent extraction.

Third, a thick ABL and/or a thick MF slows down the permeation from external water toward the sorbent and thereby increases the duration for the linear phase. To increase d_{ABL}, Chemcatcher can be put in a cage with limited openings to reduce the water flow passing the sampler. Using a thicker (non-sorbing) MF or a stack of multiple MFs should have the same effect. Thickening ABL/MF may be a simpler option than finding a high $K_{disk/w}$ sorbent, particularly for chemicals with high hydrophilicity. In this regard, the organic diffusive gradients in thin films (o-DGT) approach[27] is promising, as o-DGT devices have a thick (e.g., 750 μm) agarose gel layer which serves as a diffusive barrier toward the sorbent. Ceramic dosimeters[28] used for integrative groundwater sampling have a thick (1.5 mm) permeable ceramic layer, which also helps to linearize the uptake profile. The recent application of a microporous polyethylene tube for sampling glyphosate is based on the same idea.[29]

In this contribution we demonstrated that the 1D diffusion model can well describe the chemical uptake behavior of aqueous integrative samplers using Chemcatcher as a test case. As a mechanistic model, it can establish a direct link between physico-chemical processes and observed concentrations/masses of chemicals in the sorbent. As a result, the model was able to offer various suggestions for improvement in sampler configurations, far more useful information than mere empirical correlations of R_s and chemical properties. Extension of the model to other sampler types such as POCIS and o-DGT should be possible. Compared to the well-defined configuration of

Chemcatcher, the thickness of sorbent is unknown for these samplers, which needs to be investigated.

Associated Content

Supporting Information

More details about model parameters, initial uptake behavior of strongly sorbing compounds, comparison of partition coefficients, model results for naked and whole Chemcatchers with 12 figures and one table. This material is available free of charge via the Internet at http://pubs.acs.org.

Author Information

Corresponding author

Satoshi Endo

Phone/Fax: ++81-6-6605-2763

satoshi.endo@eng.osaka-cu.ac.jp

ORCID: 0000-0001-8702-1602

Notes

The authors declare no competing financial interest.

Author Contributions

Study design: SE. Modeling: SE, YM. Data evaluation: EV. Discussion and interpretation of results: all. Drafting of manuscript: SE. Revising manuscript: all.

Acknowledgements

The authors acknowledge the financial support from Kurita Water and Environment Foundation (15A057) and from JSPS KAKENHI Grant Number JP17K00543.

References

1. Kingston, J. K.; Greenwood, R.; Mills, G. A.; Morrison, G. M.; Persson, L. B., Development of a novel passive sampling system for the time-averaged measurement of a range of organic pollutants in aquatic environments. *J. Environ. Monit.* **2000,** *2*, (5), 487-495.
2. Alvarez, D. A.; Petty, J. D.; Huckins, J. N.; Jones-Lepp, T. L.; Getting, D. T.; Goddard, J. P.; Manahan, S. E., Development of a passive, in situ, integrative sampler for hydrophilic organic contaminants in aquatic environments. *Environ. Toxicol. Chem.* **2004,** *23*, (7), 1640-1648.
3. Vrana, B.; Allan, I. J.; Greenwood, R.; Mills, G. A.; Dominiak, E.; Svensson, K.; Knutsson, J.; Morrison, G., Passive sampling techniques for monitoring pollutants in water. *TrAC, Trends Anal. Chem.* **2005,** *24*, (10), 845-868.
4. Moschet, C.; Vermeirssen, E. L. M.; Singer, H.; Stamm, C.; Hollender, J., Evaluation of in-situ calibration of Chemcatcher passive samplers for 322 micropollutants in agricultural and urban affected rivers. *Water Res.* **2015,** *71*, 306-317.
5. Charriau, A.; Lissalde, S.; Poulier, G.; Mazzella, N.; Buzier, R.; Guibaud, G., Overview of the Chemcatcher® for the passive sampling of various pollutants in aquatic environments Part A: Principles, calibration, preparation and analysis of the sampler. *Talanta* **2016,** *148*, 556-571.
6. Vrana, B.; Mills, G. A.; Kotterman, M.; Leonards, P.; Booij, K.; Greenwood, R., Modelling and field application of the Chemcatcher passive sampler calibration data for the monitoring of hydrophobic organic pollutants in water. *Environ. Pollut.* **2007,** *145*, (3), 895-904.

7. Miller, T. H.; Baz-Lomba, J. A.; Harman, C.; Reid, M. J.; Owen, S. F.; Bury, N. R.; Thomas, K. V.; Barron, L. P., The first attempt at non-linear in silico prediction of sampling rates for polar organic chemical integrative samplers (POCIS). *Environ. Sci. Technol.* **2016,** *50*, (15), 7973-7981.
8. Harman, C.; Allan, I. J.; Bäuerlein, P. S., The challenge of exposure correction for polar passive samplers-The PRC and the POCIS. *Environ. Sci. Technol.* **2011,** *45*, (21), 9120-9121.
9. Vermeirssen, E. L. M.; Dietschweiler, C.; Escher, B. I.; van der Voet, J.; Hollender, J., Transfer kinetics of polar organic compounds over polyethersulfone membranes in the passive samplers POCIS and Chemcatcher. *Environ. Sci. Technol.* **2012,** *46*, (12), 6759-6766.
10. Gale, R. W., Three-compartment model for contaminant accumulation by semipermeable membrane Devices. *Environ. Sci. Technol.* **1998,** *32*, (15), 2292-2300.
11. Silvani, L.; Riccardi, C.; Eek, E.; Papini, M. P.; Morin, N. A. O.; Cornelissen, G.; Oen, A. M. P.; Hale, S. E., Monitoring alkylphenols in water using the polar organic chemical integrative sampler (POCIS): Determining sampling rates via the extraction of PES membranes and Oasis beads. *Chemosphere* **2017,** *184*, 1362-1371.
12. Morin, N. A. O.; Mazzella, N.; Arp, H. P. H.; Randon, J.; Camilleri, J.; Wiest, L.; Coquery, M.; Miège, C., Kinetic accumulation processes and models for 43 micropollutants in "pharmaceutical" POCIS. *Sci. Total Environ.* **2018,** *615*, 197-207.
13. Schwarzenbach, R. P.; Gschwend, P. M.; Imboden, D. M., *Environmental Organic Chemistry, 3rd ed.* John Wiley & Sons: Hoboken, 2017.
14. Lehto, N. J.; Davison, W.; Zhang, H.; Tych, W., An evaluation of DGT performance using a dynamic numerical model. *Environ. Sci. Technol.* **2006,** *40*, (20), 6368-6376.
15. Uribe, R.; Mongin, S.; Puy, J.; Cecília, J.; Galceran, J.; Zhang, H.; Davison, W., Contribution of partially labile complexes to the DGT metal flux. *Environ. Sci. Technol.* **2011,** *45*, (12), 5317-5322.

16. Endo, S.; Matsuura, Y., Characterizing sorption and permeation properties of membrane filters used for aquatic integrative passive samplers. *Environ. Sci. Technol.* **2018,** *52*, (4), 2118-2125.
17. Vermeirssen, E. L. M.; Dietschweiler, C.; Escher, B. I.; van der Voet, J.; Hollender, J., Uptake and release kinetics of 22 polar organic chemicals in the Chemcatcher passive sampler. *Anal. Bioanal. Chem.* **2013,** *405*, (15), 5225-5236.
18. Zhang, H.; Davison, W., Performance characteristics of diffusion gradients in thin films for the in situ measurement of trace metals in aqueous solution. *Anal. Chem.* **1995,** *67*, (19), 3391-3400.
19. Bayen, S.; ter Laak, T. L.; Buffle, J.; Hermens, J. L. M., Dynamic exposure of organisms and passive samplers to hydrophobic chemicals. *Environ. Sci. Technol.* **2009,** *43*, (7), 2206-2215.
20. Lohmann, R., Critical review of low-density polyethylene's partitioning and diffusion coefficients for trace organic contaminants and implications for its use as a passive sampler. *Environ. Sci. Technol.* **2012,** *46*, (2), 606-618.
21. Tran, A. T. K.; Hyne, R. V.; Doble, P., Calibration of a passive sampling device for time-integrated sampling of hydrophilic herbicides in aquatic environments. *Environ. Toxicol. Chem.* **2007,** *26*, (3), 435-443.
22. Harman, C.; Tollefsen, K. E.; Boyum, O.; Thomas, K.; Grung, M., Uptake rates of alkylphenols, PAHs and carbazoles in semipermeable membrane devices (SPMDs) and polar organic chemical integrative samplers (POCIS). *Chemosphere* **2008,** *72*, (10), 1510-1516.
23. Vermeirssen, E. L. M.; Bramaz, N.; Hollender, J.; Singer, H.; Escher, B. I., Passive sampling combined with ecotoxicological and chemical analysis of pharmaceuticals and biocides - evaluation of three Chemcatcher™ configurations. *Water Res.* **2009,** *43*, (4), 903-914.
24. Gunold, R.; Schäfer, R. B.; Paschke, A.; Schüürmann, G.; Liess, M., Calibration of the Chemcatcher® passive sampler for monitoring selected polar and semi-polar pesticides in surface water. *Environ. Pollut.* **2008,** *155*, (1), 52-60.

25. Mazzella, N.; Dubernet, J. F.; Delmas, F., Determination of kinetic and equilibrium regimes in the operation of polar organic chemical integrative samplers - Application to the passive sampling of the polar herbicides in aquatic environments. *J. Chromatogr. A* **2007,** *1154*, (1-2), 42-51.
26. Thomatou, A. A.; Zacharias, I.; Hela, D.; Konstantinou, I., Passive sampling of selected pesticides in aquatic environment using polar organic chemical integrative samplers. *Environ. Sci. Pollut. Res.* **2011,** *18*, (7), 1222-1233.
27. Chen, C.-E.; Zhang, H.; Ying, G.-G.; Jones, K. C., Evidence and Recommendations to support the use of a novel passive water sampler to quantify antibiotics in wastewaters. *Environ. Sci. Technol.* **2013,** *47*, (23), 13587-13593.
28. Martin, H.; Patterson, B. M.; Davis, G. B.; Grathwohl, P., Field trial of contaminant groundwater Monitoring: Comparing time-integrating ceramic dosimeters and conventional water sampling. *Environ. Sci. Technol.* **2003,** *37*, (7), 1360-1364.
29. Fauvelle, V.; Montero, N.; Mueller, J. F.; Banks, A.; Mazzella, N.; Kaserzon, S. L., Glyphosate and AMPA passive sampling in freshwater using a microporous polyethylene diffusion sampler. *Chemosphere* **2017,** *188*, 241-248.